HHS Public Access

Author manuscript

Cancer Res. Author manuscript; available in PMC 2019 August 15.

Published in final edited form as:

Cancer Res. 2018 August 15; 78(16): 4459–4470. doi:10.1158/0008-5472.CAN-17-3226.

Aberrant FGFR tyrosine kinase signaling enhances the Warburg effect by reprogramming LDH isoform expression and activity in prostate cancer

Junchen Liu[#1,2], **Guo Chen**[#1,2], **Zezhen Liu**[#1,2], **Shaoyou Liu**[1,2], **Zhiduan Cai**[1,2], **Pan You**[3], **Yuepeng Ke**[2], **Li Lai**[2], **Yun Huang**[2], **Hongchang Gao**[4], **Liangcai Zhao**[4], **Helene Pelicano**[5], **Peng Huang**[5], **Wallace L. McKeehan**[2], **Chin-Lee Wu**[6], **Cong Wang**[4,*], **Weide Zhong**[1,*], and **Fen Wang**[2,*]

[1]Department of Urology, Guangdong Key Laboratory of Clinical Molecular Medicine and Diagnostics, Guangzhou First People's Hospital, the Second Affiliated Hospital of South China University of Technology

[2]Institute of Biosciences and Technology, College of Medicine, Texas A&M University, Houston, TX

[3]Xianyue Hospital, Xiamen

[4]Wenzhou Medical University, Wenzhou

[5]Departments of Translational Molecular Pathology, MD Anderson Cancer Center, Houston, TX

[6]Departments of Pathology and Urology, Massachusetts General Hospital and Harvard Medical School

[#] These authors contributed equally to this work.

Abstract

The acquisition of ectopic fibroblast growth factor receptor 1 (FGFR1) expression is well documented in prostate cancer (PCa) progression. How it contributes to PCa progression is not fully understood, although it is known to confer a growth advantage and promote cell survival. Here we report that FGFR1 tyrosine kinase reprograms the energy metabolism of PCa cells by regulating expression of lactate dehydrogenase (LDH) isozymes. FGFR1 increased LDHA stability through tyrosine phosphorylation and reduced LDHB expression by promoting its promoter methylation, thereby shifting cell metabolism from oxidative phosphorylation to aerobic glycolysis. LDHA depletion compromised, whereas LDHB depletion enhanced the tumorigenicity of prostate cancer cells. Furthermore, FGFR1 overexpression and aberrant LDH isozyme expression were associated with short overall survival and biochemical recurrence times in

[*]Correspondence to Fen Wang, Institute of Biosciences and Technology, Texas A&M Health Science Center, Houston, TX 77030-3303. fwang@ibt.tamhsc.edu; Weide Zhong, Department of Urology, Guangdong Key Laboratory of Clinical Molecular Medicine and Diagnostics, Guangzhou First People's Hospital, the Second Affiliated Hospital of South China University of Technology, Guangzhou 510180, China, zhongwd2009@live.cn; or Cong Wang, Wenzhou Medical University, Wenzhou, Zhejiang, China, cwang@wmu.edu.cn.

Conflict of interests: None

patients with PCa. Our results indicate that ectopic FGFR1 expression reprograms the energy metabolism of PCa cells, representing a hallmark change in PCa progression.

Keywords

growth factor; receptor tyrosine kinase; aerobic glycolysis; prostate cancer; lactate dehydrogenase; mouse genetics

Introduction

Metabolic reprograming from oxidative phosphorylation to aerobic glycolysis is a common event in cancer progression. Although glycolysis is less efficient than oxidative phosphorylation for providing energy with respect to the number of ATP per glucose, it meets the demand of rapidly growing cancer cells for building blocks. In addition, increased glycolysis results in glucose deprivation and lactate accumulation in the tumor microenvironment, which suppresses lymphocyte infiltration and compromises anti-immunotherapies (1,2). In line with those effects, the glycolytic phenotype is associated with prostate cancer (PCa) progression and aggressiveness (3–10). An understanding of how tumor cells reprogram their metabolism from oxidative phosphorylation to aerobic glycolysis may provide a novel approach to selectively inhibit aerobic glycolysis in tumor cells.

The prostate consists of epithelial and stromal compartments, which maintain active two-way communication through paracrine mechanisms, including fibroblast growth factor (FGF) signaling in which FGF and FGF receptor (FGFR) are partitioned between the two compartments (11). That precisely balanced communication is critical for preserving the tissue homeostasis and function of the prostate. The FGF family consists of 18 ligands that exert their regulatory signals by activating the FGFR tyrosine kinases encoded by four homologous genes. FGF and FGFR are expressed throughout the body in a pattern that is spatiotemporally and cell-type specific, controlling embryonic development and maintaining adult tissue homeostasis and function.

There is extensive evidence that ectopic activation of the FGF/FGFR signaling axis are associated with PCa development and progression (11). The acquisition of ectopic FGFR1 expression stands out as the most remarkable change among the FGFR isotypes in PCa. The forced expressions of FGF and FGFR have been shown to induce prostate lesions in mouse models. On the other hand, the ablation of *Fgfr1* or *Frs2α,* which encodes FGFR-substrate 2α (FRS2α), an adaptor protein needed for FGFR kinases to activate ERK and PI3K/AKT pathways, significantly reduced PCa development and progression in mice (12,13).

FGF signaling promotes aerobic glycolysis by increasing hexokinase 2 (HK2) expression and the tyrosine phosphorylation of multiple enzymes involved in aerobic glycolysis (14). Whether and how ectopic FGF signaling contributes to PCa progression by promoting aerobic glycolysis remains to be determined. The last step of glycolysis is the reduction of pyruvate to lactate, a reversible conversion catalyzed by lactate dehydrogenase (LDH). LDH is a tetrameric enzyme composed of two types of subunits, LDHA and LDHB. The

combination of the two subunits yields five isozymes, which catalyze the conversion between pyruvate and lactate. LDH1 is composed of four LDHB subunits and favors the conversion from lactate to pyruvate, allowing oxidation along the pathway of the tricarboxylic acid cycle. LDH5 is composed of four LDHA subunits and favors the conversion from pyruvate to lactate, allowing the glycolytic pathway to be completed at the formation of lactate (15). Interestingly, hypoxia induces LDHA, while inhibits LDHB, expression (16,17). Emerging evidence shows that LDHA is required for the survival and proliferation of cancer cells. Although still a matter of debate, current data seem to indicate an association between reduced levels of LDHB and increased malignancy in PCa and other cancers (18–27).

LDHA is tyrosine phosphorylated in cancer cells (28). FGFR1 has been reported to phosphorylate LDHA at multiple tyrosine residues, which enhances tetramer formation and NADH binding and thus the enzymatic activity of LDHA (29). In this report, we demonstrate that FGFR1 signaling promotes aerobic glycolysis by stabilizing LDHA through tyrosine phosphorylation and downregulating LDHB expression through the induction of hypermethylation in the *Ldhb* promoter. We found that LDHA ablation compromised, whereas LDHB ablation enhanced, the tumorigenicity of DU145 cells. Furthermore, high levels of phosphorylated LDHA and low levels of LDHB in human PCa tissues were associated with short biochemical-recurrence and survival times in patients with PCa. Together, our results suggest that ectopically expressed FGFR1 in PCa induces metabolic changes by increasing LDHA levels and lowering LDHB levels, which promotes PCa growth and progression.

Materials and methods

Animals

Mice were housed under the Program of Animal Resources of the Institute of Biosciences and Technology in accordance with the principles and procedures of the Guide for the Care and Use of Laboratory Animals. All experimental procedures were approved by the Institutional Animal Care and Use Committee. Mice were bred and genotyped as described previously (12,30,31). For xenograft studies, 2×10^6 DU145 cells were mixed with Matrigel (BD, Biosciences, San Diego, CA) at a 1:1 ratio and subcutaneously injected into the flanks of nude mice (6 weeks old). The size of xenograft were measured with a caliper and calculated as $V=0.52 \times \text{length} \times \text{width}^2$. The xenografts were harvested after the animals were euthanized via CO_2 suffocation.

Histology

Prostate tissues and xenografts were fixed, embedded, sectioned as described (32). For immunostaining, the antigens were retrieved by boiling in citrate buffer (10 mM, pH 8.0) for 20 min. Rabbit anti-phosphorylated LDHA (pLDHA, 1:200) and anti-LDHA (1:200) were purchased from Cell Signaling Technology (Beverly, MA). Mouse anti-LDHB (1:200), rabbit anti-CD31 (1:200) and anti-Ki67 (1:200), and rat anti-F4/80 (1:200) were purchased from Abcam (Cambridge, MA). A Fluoremetric TUNEL Assay Kit was purchased from Premega Co (Fitchburg, WI). The ExtraAvidin Peroxidase System (Sigma Aldrich, St.

Louis, MO) and fluorescence-conjugated secondary antibodies (Invitrogen, Carlsbad, CA) were used to visualize specifically bound antibodies. For immunofluorescence staining, the nuclei were counterstained with To-Pro 3 before being observed under a confocal microscope (Zeiss LSM 510).

The Massachusetts General Hospital (MGH) PCa TMA was used to assess the expression of LDHA, LDHB, and Fgfr1 as well as the level of phosphorylated LDHA in human PCa samples as described (33). Immunostaining of PCa cells and that of stromal cells were evaluated separately. The percentage of positive cells was calculated and categorized as follows: 0, 0%; 1, 1–10%; 2, 11–50%; 3, 50–75%; and 4, 75–100%. The staining intensity was visually scored and defined as follows: 0, negative; 1, weak; 2, moderate; and 3, strong. Final immunoreactivity scores (IRSs) were calculated for each case by multiplying the percentage and intensity scores.

Western blotting

Cells or xenografts were homogenized in RIPA buffer as described (32). Samples containing 30 μg protein were separated by SDS-PAGE and blotted onto PVDF membranes. The anti-phosphorylated ERK1/2 (1:1,000), anti-phosphorylated AKT (1:1,000), anti-ERK1/2 (1:1,000), anti-AKT (1:1,000), anti-phosphorylated FRS2α (1:1,000), and anti-HA (1:1,000) antibodies were purchased from Santa Cruz Biotechnology (Santa Cruz, CA). Anti-pLDHA (1:1,000), anti-LDHB (1:1,000), and anti-LDHA 1:1,000) antibodies and the Glycolysis Antibody Sampler Kit containing antibodies against HK1, PFKP, PFKP2, PFKP3, aldolase, PGAM, PKM1/2, and pyruvate dehydrogenase were purchased from Cell Signaling Technology (Danvers, MA). The anti-phosphotyrosine 4G10 (1:1,000), anti-TET1 (1:1,000), and anti-Flag (1:1,000) antibodies were purchased from Millipore Sigma (Danvers, MA). The specifically bound antibodies were visualized using the ECL-Plus chemiluminescent reagents. The films were scanned with a densitometer for quantitation.

RNA expression

Total RNA was isolated from cells and tissues using the Ribopure RNA isolation reagent (Ambion, TX), reverse transcripted with SuperScript III (Life Technologies, Grand Island, NY) and random primers, and analyzed with real-time PCR using the Fast SYBR Green Master Mix (Life Technologies) as described. The results were expressed as the mean ± standard deviation as described (32). The primer sequences are listed in supplemental table 1.

Gene ablation

The lentivirus-based CRISPR-Cas9 system was used to ablate the *Ldha*, *Ldhb*, and *Fgfr1* alleles in DU145 cells. The sequences of the sgRNAs are shown in supplemental Table 1. Two days after infection with the lentivirus, the recombinant cells were selected via growth in a medium containing 2 μg/ml puromycin.

Site-directed mutagenesis

The QuikChange Lightning Multi Site-Directed Mutagenesis Kit (Agilent Technologies, Santa Clara, California) was used to generate LDHA mutant cDNAs. The primer sequences are listed in supplemental Table 1.

NMR analyses

Cells (2×10^7) were suspended in 450 μl methanol/chloroform (2:1) and lysed by ultrasound. The lysates were mixed with 450 μl chloroform/H_2O. The supernatants were lyophilized and then resuspended in 500 μl D_2O containing 0.25 mM sodium trimethylsily 1 propionate-d4. All NMR spectra were recorded on a Bruker AVANCE III 600 MHz NMR spectrometer.

MeDIP

Cells were isolated with the Qiagen Kit and ultrasound sheared into smaller fragments (200–600 bp). The sheared gDNA was denatured by incubation in 1 M NaOH/25 mM EDTA at 95°C for 12 min, and then immunoprecipitated with anti-5-methylated cytosine (5mC) antibodies. The bound 5mC-containing DNA was then purified and used to make the sequencing library with the NEB (E6240S) library prep kit, which was subsequently sequenced by the Agrelife Genomics and Bioinformatics Service, Texas A&M University.

Sodium bisulfite DNA sequence

Genomic DNA was isolated using the Qiangen Genomic DNA Kit, followed by bisulfite conversion using the EpiJET Bisulfite Conversion Kit (Thermo Scientific). The bisulfite-specific primers for the PCR amplification were listed in supplemental table 1. The PCR products were cloned into pDrive Cloning Vectors (Qiangen) and sequenced.

Protein stability assay

Stable MEF transfectants expressing HA-tagged LDHA were treated with cycloheximide for the indicated times. The abundance of LDHA was examined by Western blot. The relative level of endogenous or HA-tagged LDHA was quantitated using Image J. The GraphPad software was used to compare the slopes of each curve.

Statistical analysis

Statistical analysis was performed using the two-tailed t test. For protein stability assay, the GraphPad software was used to compare two curves. $P < 0.05$ is considered statistical significant. Error bars indicate standard deviations.

Results

Ablation of the FGF signaling axis reduces glycolysis and increases oxygen consumption in mouse embryonic fibroblasts (MEFs)

We first determined whether FGF signaling regulated cell metabolism in MEFs, which expressed FGFR1, FGFR2, and FRS2α. We generated MEFs that were devoid of *Fgfr1*, *Fgfr2*, and *Frs2α* by infecting MEFs bearing floxed *Fgfr1*, *Fgfr2*, and *Frs2α* alleles with

adenovirus carrying the Cre-GFP coding sequence. The cells, designated MEF$^{\Delta F}$, did not express *Fgfr1*, *Fgfr2*, and *Frs2α* mRNA (Fig. 1A). Interestingly, real-time RT-PCR also revealed that at the mRNA level, MEF$^{\Delta F}$ increased *Ldhb*, but not *Ldha* expression. However, western blots revealed that at the protein level, compared with parental MEFs, the MEF$^{\Delta F}$ cells had reduced LDHA expression and increased LDHB expression (Fig. 1B). Those results suggest that FGF signaling promotes LDHA expression at the protein level and suppresses LDHB expression at the mRNA level. Western blot also showed that FGF2 failed to induce phosphorylation of FRS2α, ERK, and AKT, indicating successful abrogation of FGF signaling in the cells.

LDHA and LDHB favor opposite direction of the conversation between pyruvate and lactate (15). To determine whether abrogation of the FGF signaling axis in MEFs changes the cell metabolism, we compared the lactate production and oxygen consumption in MEFs and MEF$^{\Delta F}$ cells (Fig. 1C). The abrogation of FGF signaling reduced lactate production and increased the oxygen consumption rate. In contrast, overexpression of LDHA in MEF$^{\Delta F}$ cells significantly increased lactate production (Fig. S1). In addition, NMR analyses revealed that the abrogation of FGF signaling reduced the concentrations of isoleucine, valine, lactate, and acetate and increased the concentrations of glutamate and succinate (Fig. 1D). The reduced isoleucine and valine levels in MEF$^{\Delta F}$ cells suggests that the synthesis of branched chain amino acids (BCAAs) was compromised. The dysregulation of BCAA synthesis in MEFs lacking FGF signaling is in line with evidence that BCAAs promote glucose uptake (34). Those results demonstrate a shift in energy metabolism from aerobic glycolysis to oxidative phosphorylation in MEF$^{\Delta F}$ cells, suggesting that energy metabolism in MEFs is regulated by FGF signaling.

FGFR1 enhances the stability of LDHA via tyrosine phosphorylation

To determine the role of FGFR1 in the regulation of LDHA at the protein level, we treated the MEFs and MEF$^{\Delta F}$ cells with cycloheximine to block protein synthesis. Western blots revealed that the abundance of LDHA declined faster in MEF$^{\Delta F}$ cells than in the parental MEFs (Fig. 2A). Those results indicate that the half-life of LDHA is shorter in MEF$^{\Delta F}$ cells than in the parental MEFs, suggesting that FGF signaling enhances the stability of LDHA.

LDHA consists of four tyrosine-phosphorylation sites (Fig. 2B). In line with a previous report that FGFR1 directly phosphorylates LDHA (29), western blots with the anti-phosphotyrosine antibody 4G10 showed that LDHA was tyrosine phosphorylated (Fig. 2C). To identify which tyrosine-phosphorylation sites were involved in the regulation of LDHA stability, we employed site-directed mutagenesis to generate LDHA mutants with individual, double (2F), or quadruple (4F) mutations. The individual mutations at each of the four tyrosine-phosphorylation sites did not affect the phosporylation LDHA. Note that weak expression of FGFR1 in the Y83F group might account for the relatively low phosphorylation of Y83F. Only the 4F mutant failed to be phosphorylated by FGFR1. The other mutants displayed only partially reduced phosphorylation, comfirming the previous report that all four tyrosine residues are phosphorylated by FGFR1.

Western blot analyses revealed that the individual mutations at each of the four tyrosine-phosphorylation sites and the two 2F mutants did not affect the stablility of LDHA ($P>0.05$).

However, the 4F mutant showed a statistically significant reduction in stabilitity (Fig. 2D). Together, those results indicate that phosphorylation of the four tyrosine residues promotes the stability of LDHA.

FGFR1 suppresses LDHB transcription by promoting DNA methylation in the LDHB promoter

The *Ldhb* promoter is heavily methylated in PCa, which inhibits the transcription of LDHB (22). To determine whether FGF signaling suppresses LDHB expression via promoter methylation, we employed methylated DNA immunoprecipitation (MeDIP) to pull down the methylated DNA for high-throughput sequencing (Fig. 3A). The results showed that the CpG islands in the *Ldhb* promoter were less methylated in $MEF^{\Delta F}$ cells than in the parental MEFs. Further bisulfite sequencing of the *Ldhb* promoter area confirmed that DNA demethylation was reduced in the $MEF^{\Delta F}$ cells (Fig. 3B). Consistent with the data that ablation of FGF signaling did not affect LDHA mRNA expression, no differences were observed in *ldha* promoter methylation between MEF and $MEF^{\Delta F}$ cells (Fig. S2).

Because DNA demethylation is catalyzed by the three TET enzymes (TET1–3), we compared the expression levels of TET1–3 in $MEF^{\Delta F}$ cells and parental MEFs. We found that the expression of *Tet1* at both mRNA and protein levels was significantly increased in the $MEF^{\Delta F}$ cells (Fig. 3C&D), suggesting that FGF signaling suppressed *Tet1* expression. Consistantly, *Ldhb*, but not *ldha*, expression was higher in MEFs bearing $Tet1^{null}$ alleles than in parental MEFs (Fig. 3E), further indicating that the expression of LDHB was reduced by DNA methylation.

Ablation of the FGF signaling axis reprograms cell metabolism in human PCa cells

DU145 cells highly expressed Fgfr1 (Fig. 4A). To investigate whether ectopic FGF signaling contributes to metabolic reprogramming in PCa, we used CRISPR/Cas9 gene editing to ablate the *Fgfr1* alleles in DU145 cells that expressed high levels FGFR1. Although it did not affect cell growth in the medium with 10% FBS, ablation of *Fgfr1* compromised cell growth in the medium with 1% serum (Fig. S3). In line with the data from MEFs, the expression of *Ldha* mRNA was not affected in the $Fgfr1^{null}$ DU145 ($DU145^{\Delta R1}$) cells, whereas that of *Ldhb* mRNA was increased (Fig. 4B). We then determined the expression profiles of the LDH isozymes in the parental and $DU145^{\Delta R1}$ cells by western blot (Fig. 4C). The ablation of *Fgfr1* reduced LDHA expression and increased LDHB expression at the protein level. Interestingly, expression of FGFR1 protein was increased by FGF2 treatment. However, the underlying mechanism remains to be determined. Together with Fig. 4B, the results further indicate that FGFR1 regulates LDHA at either the translational or posttranslational level and LDHB at the transcriptional level. Consistent with the report that FGFR1 phosphorylates LDHA, western blots revealed that the phosphorylation of LDHA at the Y10 residue was reduced in the $DU145^{\Delta R1}$ cells. Consistently, the ablation of *Fgfr1* reduced glucose uptake and lactate production and increased O_2 consumption (Fig. 4D). Similarly, treating DU145 cells with FGFR inhibitor AZD4547 also suppressed glycolysis (Fig. S4). Together, the data suggest that the ablation of *Fgfr1* in PCa cells reprograms the cell energy metabolism from oxidative phosphorylation to aerobic glycolysis.

LDHA ablation reduces, whereas LDHB ablation enhances, the tumorigenesis of DU145 cells

To investigate the functions of the LDH isoforms in the tumorigenic activity of PCa cells, we employed CRISPR/Cas9 to delete the *Ldha* or *Ldhb* alleles in DU145 cells, designated DU145$^{\Delta Ldha}$ and DU145$^{\Delta Ldhb}$, respectively. Western blot analyses of the xenografts revealed that the ablation of *Ldha* increased PGAM levels, while the ablation of *Ldhb* increased HK1, PFK3, and aldolase levels (Fig. 5A). Those results indicate that LDHA depletion compromised, whereas LDHB depletion enhanced, glycolysis in DU145 cells. Although no difference was observed in growth rates (Fig. 5B), when grafted subcutaneously into the flanks of nude mice, DU145$^{\Delta Ldha}$ cells generated smaller tumors compared with parental DU145 cells (Fig. 5C). In contrast, grafts of DU145$^{\Delta Ldhb}$ cells generated larger tumors than those of parental DU145 cells. Consistantly, similar results were derived from PC3 cells (Fig. S5).

LDHA deletion and LDHB deletion both stimulated compensatory upregulation of glycolytic-related proteins but had opposite effects on tumor growth, suggesting that there might be unidentified proteins that mediate LDH-regulated tumor growth. Noticebly, ablation of *Ldha* increased expression of LDHB and vice versa. Whether this changes is due to feedback regulation to compensate the loss of LDH remains to be investigated.

Although there were no significant differences in tissue histology among the parental DU145, DU145$^{\Delta Ldha}$, and DU145$^{\Delta Ldhb}$ xenografts, the DU145$^{\Delta Ldha}$ xenografts had less, and the DU145$^{\Delta ldhb}$ xenografts had more, Ki67^{+} cells than the parental DU145 xenografts, indicating that the ablation of *Ldha* reduced, and the ablation of *Ldhb* increased, the number of proliferating cells in the xenografts (Fig. 6A&B). Furthermore, there were more apoptotic cells in the DU145$^{\Delta Ldha}$ xenografts than in the parental DU145 xenografts, whereas the opposite relation was observed between the DU145$^{\Delta Ldhb}$ xenografts and the parental DU145 xenografts (Fig. 6C). To investigate the impact of *Ldha* or *Ldhb* ablation on the tumor microenvironment, we stained DU145$^{\Delta Ldha}$, DU145$^{\Delta Ldhb}$, and parental DU145 xenografts with anti-CD31 antibodies and anti-F4/80 antibodies to examine the densities of microvessels and macrophages, respectively. There were fewer CD31^{+} and F4/80^{+} cells in the DU145$^{\Delta Ldha}$ xenografts than in the parental DU145 xenografts. In contrast, there were more CD31^{+} and F4/80^{+} cells in the DU145$^{\Delta Ldhb}$ xenografts than in the parental DU145 xenografts. Those results demonstrated that *Ldha* ablation compromised, whereas *Ldhb* ablation stimulated, angiogenesis and macrophage infiltration and thus the tumorigenic activity of DU145 cells.

Hyperphosphorylation of LDHA and reduced LDHB expression levels in human PCa

We performed immunohistochemical staining to determine the expression patterns of LDHA and LDHB in a human prostate tissue microarray (TMA) that comprised 225 PCa samples and 27 benign prostate samples (33). The results suggested that LDHA levels were higher in PCa tissues than in adjacent prostate tissues (Fig. 7A). FGFR1 can phosphorylate human LDHA at multiple tyrosine residues (29). Compared with non-cancerous tissues, PCa tissues had higher levels of Y10-phosphorylated LDHA (pLDHA) and lower levels of LDHB (Fig. 7B).

The samples in the TMA were annotated with detailed information based on a 15-year follow-up of the patients, including PSA recurrence, Gleason Scores, pathological stages, patients' age, and survival time. Therefore, we separated the samples into two groups based on the median level. Higher than the median is defined as High and lower than the median is defined as Low. As shown in Fig. 7C&D, the clinical outcomes of the patients with high pLDHA levels (N=153) were worse than those of the patients with low pLDHA levels (N=48), while those of patients with low LDHB levels (N=126) were worse than those of patients with high LDHB levels (N=96); the patients with high pLDHA levels and low LDHB levels (N=13) clearly had shorter biochemical recurrence-free times than those with low pLDHA levels and high LDHB levels (N=86). Those results suggest that pLDHA and LDHB expression have the potential to serve as biomarkers for PCa prognosis.

Fgfr1 is overexpressed in about 40% of human PCas (35,36). To determine whether the expression level of *Fgfr1* correlates with the abundance of pLDHA, we used *in situ* hybridization to assess the expression levels of *Fgfr1* in the TMA. *Fgfr1* expressed was higher in PCa than in benign tissues (Fig. 7D). The expression was associated with short PSA-free survival time (Fig. 7E). Furthermore, the *Fgfr1* expression level was positively associated with the level of pLDHA (Fig. 7F). Together, the data imply that ectopically expressed *Fgfr1* in PCa deregulates the expression of LDH isozymes and thus changes the glycolysis and metabolism of the cells (Fig. 7G).

Discussion

There is extensive evidence that ectopic FGF/FGFR1 signaling is a contributing factor in PCa development and progression (11,36–41), that FGF-mediated glycolysis plays a pivotal role in development (14,42), and that FGFR1 directly phosphorylates LDHA and enhances its enzymatic activity (29). Herein we showed that FGFR1 signaling promotes aerobic glycolysis by upregulating LDHA at the protein level and downregulating LDHB at the transcriptional level. The ablation of LDHA compromised, whereas that of LDHB enhanced, the tumorigenic activity of DU145 PCa cells. Furthermore, high levels of phosphorylated LDHA and low levels of LDHB in human PCa tissues were associated with short biochemical-recurrence and survival times of patients. Our results suggest that ectopic FGFR1 signaling contributes to PCa progression by reprograming cell energy metabolism and that high levels of phosphorylated LDHA and high expression levels of LDHB are potential biomarkers for PCa diagnosis and prognosis.

LDHA has four tyrosine-phosphorylation sites. Phosphorylation at tyrosine 10 enhances the formation of tetramers and increases enzymatic activity, while phosphorylation at tyrosine 83 enhances the binding of NADH (29). In addition, high levels of FGFR1 expression are associated with high levels of phosphorylated LDHA (43). Tyrosine 10 only exists in human LDHA, suggesting that Y10 phosphorylation is not the only way in which FGFR1 activates LDHA. We showed that phosphorylation of the four tyrosine-phosphorylation sites by FGFR1 extended the half-life of LDHA. Ablation of the FGF signaling axis significantly reduced the half-life of LDHA; the substitution of phenylalanine at the four tyrosine residues in LDHA had the same effect (Fig. 2). Together, the results suggest that tyrosine phosphorylation not only increases the enzymatic activity of LDHA but also enhances the

stability of LDHA. More research is needed to determine how tyrosine phosphorylation affects the half-life of LDHA.

It has been reported that LDHB expression is silenced by hypermethylation of the *LDHB* promoter in human PCa (23). We found that *Fgfr1* ablation reduced the methylation of CpG islands in the *Ldhb* promoter (Fig. 3A&B). The ablation of FGF signaling in MEFs increased the expression of *Tet1*, which catalyzes the conversion of methylated guanidine to hydroxyl-methylated guanidine, the first step of DNA demethylation. Moreover, ablation of *Tet1* increased LDHB expression although ablation of LDHA or LDHB did not affect TET1 expression (Fig. S6). Thus, our results demonstrate that FGF signaling suppresses LDHB expression by promoting *Tet1* expression.

Since LDHA promotes aerobic glycolysis while LDHB facilitates oxidative phosphorylation, LDHA may enhance tumor progression by fueling aerobic glycolysis and LDHB exerts opposite effects in glycolytic PCa cells. Our results in Fig. 4 revealed that LDHA and LDHB have opposite effects on PCa growth further support this hypothesis. Hence, it is essential to develop new strategies to specifically inhibit LDHA without compromising LDHB activity. FGFR1 selectively phosphorylates LDHA on multiple tyrosine residues, which stabilizes LDHA, and concurrently enhances the expression of LDHB. Yet, other signaling pathways may also regulate cell metabolism, which may explain why ablation of FGF signaling did not fully convert LDH expression from LDHA to LDHB. It has been reported that LDHA is degraded via chaperone-mediated autophagy (44). However, no difference in LDHA degradation was observed in DU145 and DU145$^{\Delta R1}$ cells with or without treating with protease inhibitor leupeptin or autophagy inhibitor biflomycin (Fig. S7), suggesting that FGF signaling protected LDHA degradation via other mechanism. Although both lactate production and glucose consumption are reduced in DU145$^{\Delta R1}$ cells (Fig. 4), the growth curves of DU145 and DU145$^{\Delta R1}$ were not significantly different in glucose-free medium with or without lactate supplement, suggesting that deletion of FGFR1 did not confer the cells ability to use lactate as a main energy source. Further efforts are warranted to fully understand how cell metabolism is regulated.

Our data are consistent with reports that loss of LDHB correlated with malignancy (20,26,45). However, it is different from the report that LDHB expression is associated with poor survival in uterine cancer patients (27,46). One explanation is that in the cancer, such as uterine cancer, that largely rely on the TCA cycle to fuel cellular activities, can be inhibited by LDHB depletion. In other cancers, such as metastatic PCa, however, rely on aerobic glycolysis, and therefore, is benefited from LDHB depletion. Therefore, more studies are needed to understand the role of LDHB in various types of malignancies. Our data show that although the deletion of FGFRs led to an increase in oxygen consumption, it still reduced ATP production. These results suggest that the upregulation of oxidative phosphorylation is not sufficient to make up the energy loss due to FGFR ablation, and that PCa cells derive ATP primarily from aerobic glycolysis.

Although FRS2α is required for the FGF kinase to activate the ERK and PI3K/AKT pathways, we found that deletion of *Frs2α* alleles did not affect LDHA and LDHB expression as well as lactate production in MEFs (Fig. S8). This is consistent with the fact

that FGFR1 directly phosphorylates LDHA. The mechanism by which FGF signaling regulates LDHB promoter methylation remains to be determined.

In summary, we demonstrated that FGF signaling promotes aerobic glycolysis and that ectopic FGF signaling in PCa reprograms cell metabolism, suppressing aerobic glycolysis and promoting oxidative phosphorylation. LDHA deletion suppressed, whereas LDHB deletion promoted, the tumorigenic activity of PCa cells. Furthermore, the LDHA overexpression and LDHB downregulation correlated with short biochemical-recurrence and survival times in patients with PCa. Our results shed new light on how the manipulation of ectopic FGF signaling may serve as a strategy for PCa treatment.

Supplementary Material

Refer to Web version on PubMed Central for supplementary material.

Acknowledgement

We thank Drs. Juha Patanen and David Ornitz for sharing the *Fgfr1*^{floxed} and *Fgfr2*^{floxed} mice, respectively.

Financial Support: This work was supported by the NIH CA96824, TAMU1400302, CPRIT 110555 grants, and a gift from Agilent Technology, Inc. to F Wang, the National Natural Science Foundation of China 81101712, 31371470, and 81270761 grants to C Wang; and National Key Basic Research Program of China (2015CB553706), National Natural Science Foundation of China (81571427) and the Fundamental Research Funds for the Central Universities (2017PY023) to WD Zhong.

REFERENCES

1. FischerKHoffmannPVoelklSMeidenbauerNAmmerJEdingerM, et al. Inhibitory effect of tumor cell-derived lactic acid on human T cells. Blood 2007;109:3812–9 [PubMed: 17255361]
2. BrandASingerKKoehlGEKolitzusMSchoenhammerGThielA, et al. LDHA-Associated Lactic Acid Production Blunts Tumor Immunosurveillance by T and NK Cells. Cell Metab 2016
3. CiccareseCSantoniMMassariFModenaAPivaFContiA, et al. Metabolic Alterations in Renal and Prostate Cancer. Curr Drug Metab 2015
4. XianZYLiuJMChenQKChenHZYeCJXueJ, et al. Inhibition of LDHA suppresses tumor progression in prostate cancer. Tumour Biol 2015;36:8093–100 [PubMed: 25983002]
5. Pertega-GomesNFelisbinoSMassieCEVizcainoJRCoelhoRSandiC, et al. A glycolytic phenotype is associated with prostate cancer progression and aggressiveness: a role for monocarboxylate transporters as metabolic targets for therapy. J Pathol 2015;236:517–30 [PubMed: 25875424]
6. MrazJVrubelFHanselovaM Carcinoma of the prostate. II. Serum activity of acid phosphatase, prostatic acid phosphatase, LDH and its isoenzymes. Int Urol Nephrol 1979;11:301–9 [PubMed: 536179]
7. VrubelFMrazJNemecekRPapousekFHanselovaM Carcinoma of the prostate. I. Histochemical examination as an aid in evaluating prostate carcinoma. Int Urol Nephrol 1979;11:295–9 [PubMed: 536178]
8. OliverJAel-HilaliMMBelitskyPMacKinnonKJ LDH isoenzymes in benign and malignant prostate tissue. The LDH V-I ratio as an index of malignancy. Cancer 1970;25:863–6 [PubMed: 4191903]
9. NaruseKYamadaYAokiSTakiTNakamuraKTobiumeM, et al. Lactate dehydrogenase is a prognostic indicator for prostate cancer patients with bone metastasis. Hinyokika Kiyo 2007;53:287–92 [PubMed: 17561711]
10. KeshariKRSriramRVan CriekingeMWilsonDMWangZJVigneronDB, et al. Metabolic reprogramming and validation of hyperpolarized 13C lactate as a prostate cancer biomarker using a human prostate tissue slice culture bioreactor. Prostate 2013;73:1171–81 [PubMed: 23532911]

11. WangFLuoYMcKeehanW The FGF signaling axis in prostate tumorigenesis . In: GESCRF, editors. Molecular Oncology: Causes of Cancer and Targets for Treatment. London Cambridge University Press; 2013 p 186–9.
12. ZhangYZhangJLinYLanYLinCXuanJW, et al. Role of epithelial cell fibroblast growth factor receptor substrate 2{alpha} in prostate development, regeneration and tumorigenesis. Development 2008;135:775–84 [PubMed: 18184727]
13. YangFZhangYResslerSJIttmannMMAyalaGEDangTD, et al. FGFR1 is essential for prostate cancer progression and metastasis. Cancer Res 2013;73:3716–24 [PubMed: 23576558]
14. YuPWilhelmKDubracATungJKAlvesTCFangJS, et al. FGF-dependent metabolic control of vascular development. Nature 2017
15. FritzPJ Rabbit muscle lactate dehydrogenase 5; a regulatory enzyme. Science 1965;150:364–6 [PubMed: 4284206]
16. SemenzaGLJiangBHLeungSWPassantinoRConcordetJPMaireP, et al. Hypoxia response elements in the aldolase A, enolase 1, and lactate dehydrogenase A gene promoters contain essential binding sites for hypoxia-inducible factor 1. J Biol Chem 1996;271:32529–37 [PubMed: 8955077]
17. LiangXLiuLFuTZhouQZhouDXiaoL, et al. Exercise Inducible Lactate Dehydrogenase B Regulates Mitochondrial Function in Skeletal Muscle. J Biol Chem 2016;291:25306–18 [PubMed: 27738103]
18. DennisonJBMolinaJRMitraSGonzalez-AnguloAMBalkoJMKubaMG, et al. Lactate dehydrogenase B: a metabolic marker of response to neoadjuvant chemotherapy in breast cancer. Clin Cancer Res 2013;19:3703–13 [PubMed: 23697991]
19. McClelandMLAdlerASDemingLCosinoELeeLBlackwoodEM, et al. Lactate dehydrogenase B is required for the growth of KRAS-dependent lung adenocarcinomas. Clin Cancer Res 2013;19:773–84 [PubMed: 23224736]
20. McClelandMLAdlerASShangYHunsakerTTruongTPetersonD, et al. An integrated genomic screen identifies LDHB as an essential gene for triple-negative breast cancer. Cancer Res 2012;72:5812–23 [PubMed: 23139210]
21. ZhaXWangFWangYHeSJingYWuX, et al. Lactate dehydrogenase B is critical for hyperactive mTOR-mediated tumorigenesis. Cancer Res 2011;71:13–8 [PubMed: 21199794]
22. MaekawaMTaniguchiTIshikawaJSugimuraHSuganoKKannoT Promoter hypermethylation in cancer silences LDHB, eliminating lactate dehydrogenase isoenzymes 1–4. Clin Chem 2003;49:1518–20 [PubMed: 12928234]
23. LeiblichACrossSSCattoJWPhillipsJTLeungHYHamdyFC, et al. Lactate dehydrogenase-B is silenced by promoter hypermethylation in human prostate cancer. Oncogene 2006;25:2953–60 [PubMed: 16547507]
24. CuiJQuanMJiangWHuHJiaoFLiN, et al. Suppressed expression of LDHB promotes pancreatic cancer progression via inducing glycolytic phenotype. Med Oncol 2015;32:143 [PubMed: 25807933]
25. KimJHKimELLeeYKParkCBKimBWWangHJ, et al. Decreased lactate dehydrogenase B expression enhances claudin 1-mediated hepatoma cell invasiveness via mitochondrial defects. Exp Cell Res 2011;317:1108–18 [PubMed: 21356207]
26. ChenRZhouXYuZLiuJHuangG Low Expression of LDHB Correlates With Unfavorable Survival in Hepatocellular Carcinoma: Strobe-Compliant Article. Medicine (Baltimore) 2015;94:e1583 [PubMed: 26426634]
27. BrissonLBanskiPSboarinaMDethierCDanhierPFontenilleMJ, et al. Lactate Dehydrogenase B Controls Lysosome Activity and Autophagy in Cancer. Cancer Cell 2016;30:418–31 [PubMed: 27622334]
28. LiSSPanYESharIefFSEvansMJLinMFClintonGM, et al. Cancer-associated lactate dehydrogenase is a tyrosylphosphorylated form of human LDH-A, skeletal muscle isoenzyme. Cancer Invest 1988;6:93–101 [PubMed: 3365574]
29. FanJHitosugiTChungTWXieJGeQGuTL, et al. Tyrosine phosphorylation of lactate dehydrogenase A is important for NADH/NAD(+) redox homeostasis in cancer cells. Mol Cell Biol 2011;31:4938–50 [PubMed: 21969607]

30. LinYLiuGZhangYHuYPYuKLinC, et al. Fibroblast growth factor receptor 2 tyrosine kinase is required for prostatic morphogenesis and the acquisition of strict androgen dependency for adult tissue homeostasis. Development 2007;134:723–34 [PubMed: 17215304]
31. WangCChangJYYangCHuangYLiuJYouP, et al. Type 1 fibroblast growth factor receptor in cranial neural crest cells-derived mesenchyme is required for palatogenesis. J Biol Chem 2013
32. HuangYJinCHamanaTLiuJWangCAnL, et al. Overexpression of FGF9 in Prostate Epithelial Cells Augments Reactive Stroma Formation and Promotes Prostate Cancer Progression. Int J Biol Sci 2015;11:948–60 [PubMed: 26157349]
33. ZhongWDLiangYXLinSXLiLHeHCBiXC, et al. Expression of CD147 is associated with prostate cancer progression. Int J Cancer 2012;130:300–8 [PubMed: 21328337]
34. NishitaniSTakehanaKFujitaniSSonakaI Branched-chain amino acids improve glucose metabolism in rats with liver cirrhosis. Am J Physiol Gastrointest Liver Physiol 2005;288:G1292–300 [PubMed: 15591158]
35. AcevedoVDGangulaRDFreemanKWLiRZhangYWangF, et al. Inducible FGFR-1 activation leads to irreversible prostate adenocarcinoma and an epithelial-to-mesenchymal transition. Cancer Cell 2007;12:559–71 [PubMed: 18068632]
36. OzenMGiriDRopiquetFMansukhaniAIttmannM Role of fibroblast growth factor receptor signaling in prostate cancer cell survival. J Natl Cancer Inst 2001;93:1783–90 [PubMed: 11734594]
37. Abate-ShenCShenMM FGF signaling in prostate tumorigenesis--new insights into epithelial-stromal interactions. Cancer Cell 2007;12:495–7 [PubMed: 18068626]
38. TaylorBSSchultzNHieronymusHGopalanAXiaoYCarverBS, et al. Integrative genomic profiling of human prostate cancer. Cancer Cell 2010;18:11–22 [PubMed: 20579941]
39. GiriDRopiquetFIttmannM Alterations in expression of basic fibroblast growth factor (FGF) 2 and its receptor FGFR-1 in human prostate cancer. Clin Cancer Res 1999;5:1063–71. [PubMed: 10353739]
40. DevilardEBladouFRamuzOKarsentyGDalesJPGravisG, et al. FGFR1 and WT1 are markers of human prostate cancer progression. BMC Cancer 2006;6:272 [PubMed: 17137506]
41. WangJStocktonDWIttmannM The fibroblast growth factor receptor-4 Arg388 allele is associated with prostate cancer initiation and progression. Clin Cancer Res 2004;10:6169–78 [PubMed: 15448004]
42. SugiuraKSuYQDiazFJPangasSASharmaSWigglesworthK, et al. Oocyte-derived BMP15 and FGFs cooperate to promote glycolysis in cumulus cells. Development 2007;134:2593–603 [PubMed: 17553902]
43. JinLChunJPanCAlesiGNLiDMaglioccaKR, et al. Phosphorylation-mediated activation of LDHA promotes cancer cell invasion and tumour metastasis. Oncogene 2017
44. ZhaoDZouSWLiuYZhouXMoYWangP, et al. Lysine-5 acetylation negatively regulates lactate dehydrogenase A and is decreased in pancreatic cancer. Cancer Cell 2013;23:464–76 [PubMed: 23523103]
45. KohYWLeeSJParkSY Prognostic significance of lactate dehydrogenase B according to histologic type of non-small-cell lung cancer and its association with serum lactate dehydrogenase. Pathol Res Pract 2017;213:1134–8 [PubMed: 28756978]
46. LiCChenYBaiPWangJLiuZWangT, et al. LDHB may be a significant predictor of poor prognosis in osteosarcoma. Am J Transl Res 2016;8:4831–43 [PubMed: 27904684]

Significance: FGF signaling drives the Warburg effect through differential regulation of LDHA and LDHB, thereby promoting the progression of prostate cancer.

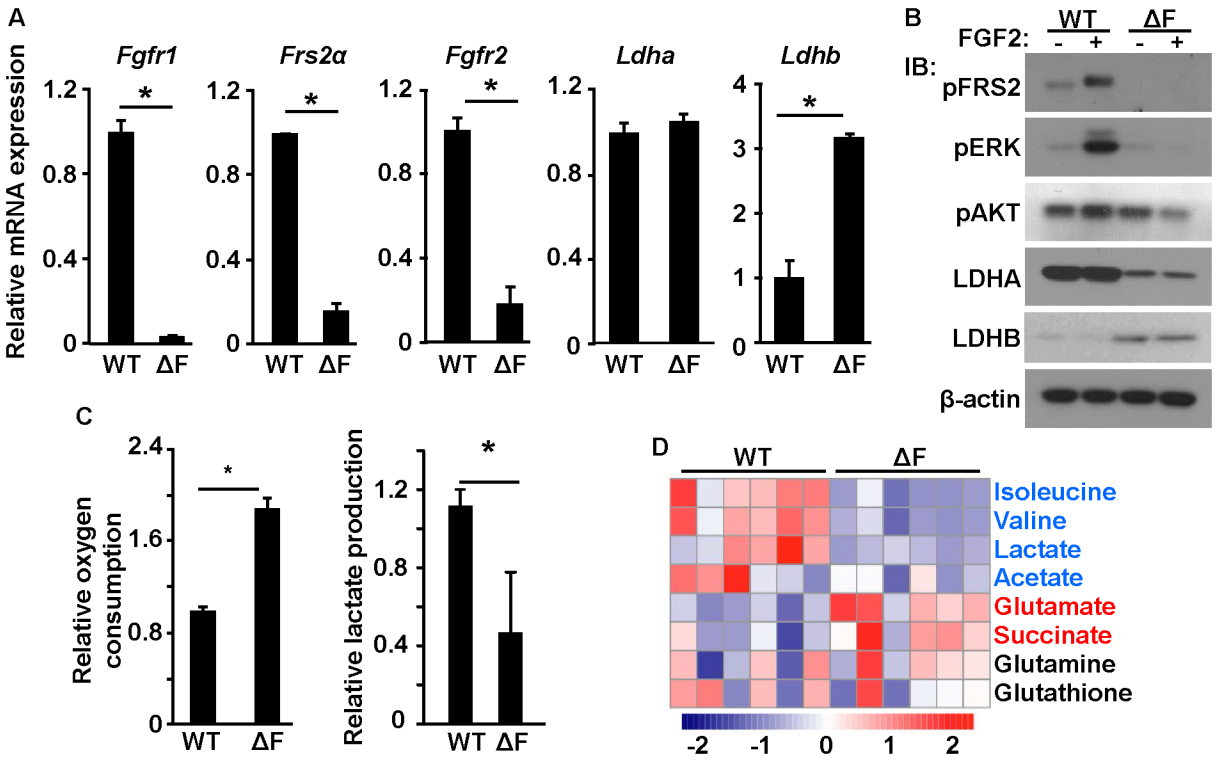

Fig. 1. Ablation of FGF signaling suppresses aerobic glycolysis and promotes oxidative phosphorylation in MEFs

A. Real-time RT-PCR analyses of the indicated mRNAs. **B.** Western blot of the indicated proteins. **C.** Relative oxygen consumption and lactate production. **D.** NMR analyses demonstrated metabolite changes in $MEF^{\Delta F}$ cells. Each column represent an individual sample. WT, wildtype; Ctrl, control; ΔF, $MEF^{\Delta F}$; *, P<0.05.

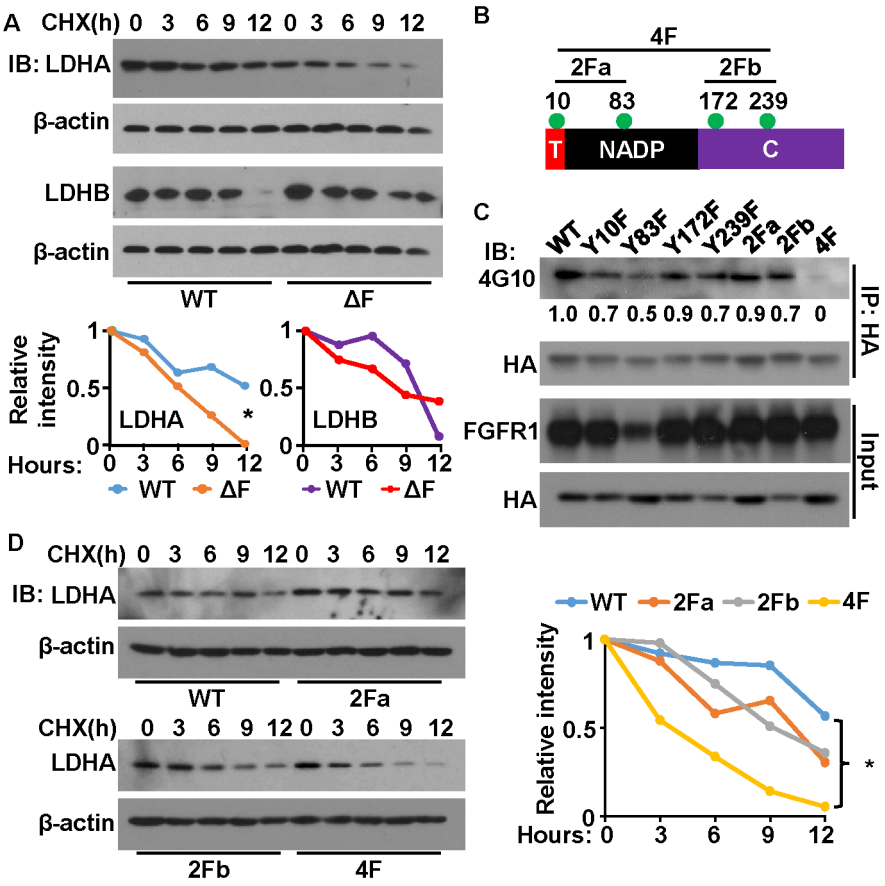

Fig. 2. Tyrosine phosphorylation suppresses the degradation of LDHA

A. The cells were treated with cycloheximide for the indicated times. Endogenous LDHA proteins were determined by western blot. The intensity of LDHA relative to that of β-actin was shown on the right panel. **B.** The structural domains of LDHA. Green dots indicate the tyrosine-phosphorylation sites. **C**. HA-tagged LDHA was expressed in 239T cells with FGFR1. Phosphorylated LDHA was detected with anti-phosphotyrosine antibody 4G10. **D**. The cells were treated with cycloheximide (CHX) for the indicated times. The levels of LDHA were determined by western blot. The intensity of LDHA relative to that of β-actin was shown on the right panel. T, tetramer formation domain; NADP, NAD/NADP binding domain; C, C-terminal domain; 2Fa, Y10F/Y83F mutation; 2Fb, Y172/Y239 mutation; 4F, Y10F/Y83F/Y172/Y239 mutation; IP, immunoprecipitation; IB, immunoblot; *, $P < 0.01$.

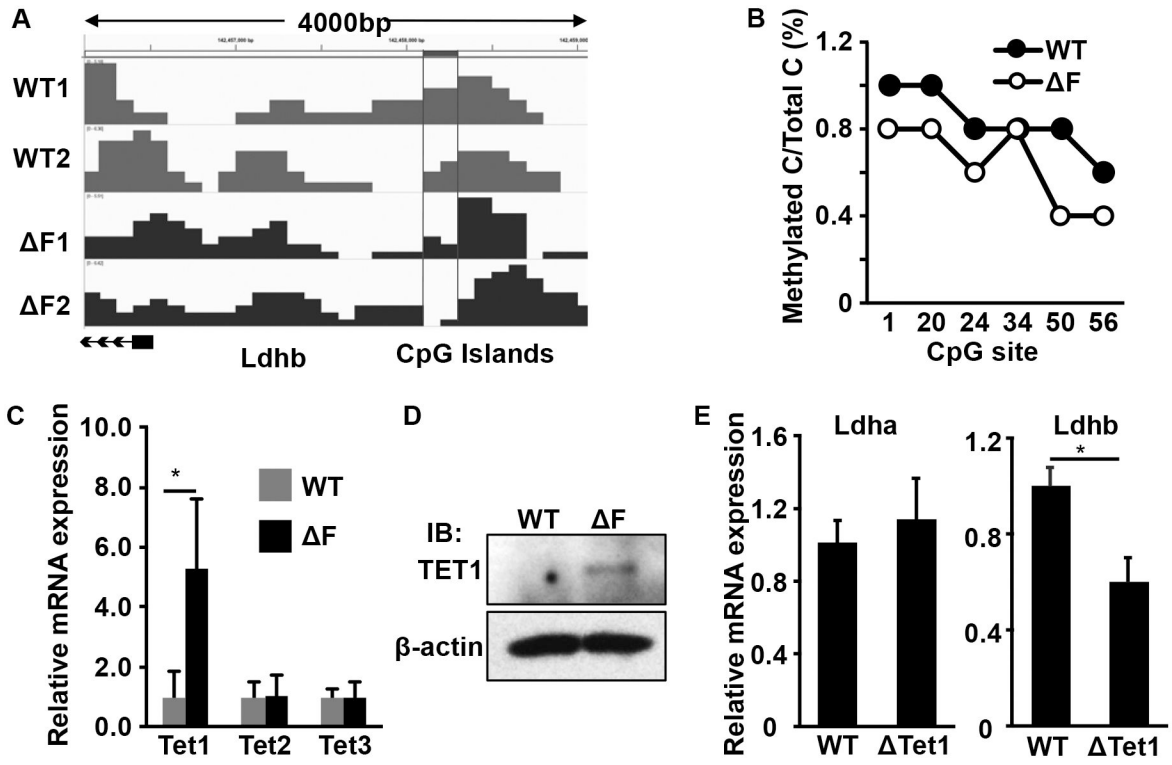

Fig. 3. Ablation of FGF signaling reduces DNA methylation in the *Ldhb* promoter

A. Methylated DNA was immunoprecipitated and subjected to high-throughput sequencing. The level of methylation at CpG islands in the *Ldhb* promoter region is shown. **B.** Bisulfite DNA sequencing of the *Ldhb* promoter area in $MEF^{\Delta F}$ cells. **C&D.** Real-time RT-PCR and western blot analyses showing increased Tet1 in $MEF^{\Delta F}$ cells at the mRNA and protein levels. **E.** Real-time RT-PCR analyses of *ldha* and *Ldhb* in *Tet1* null MEF (ΔTet1). *, $P < 0.05$.

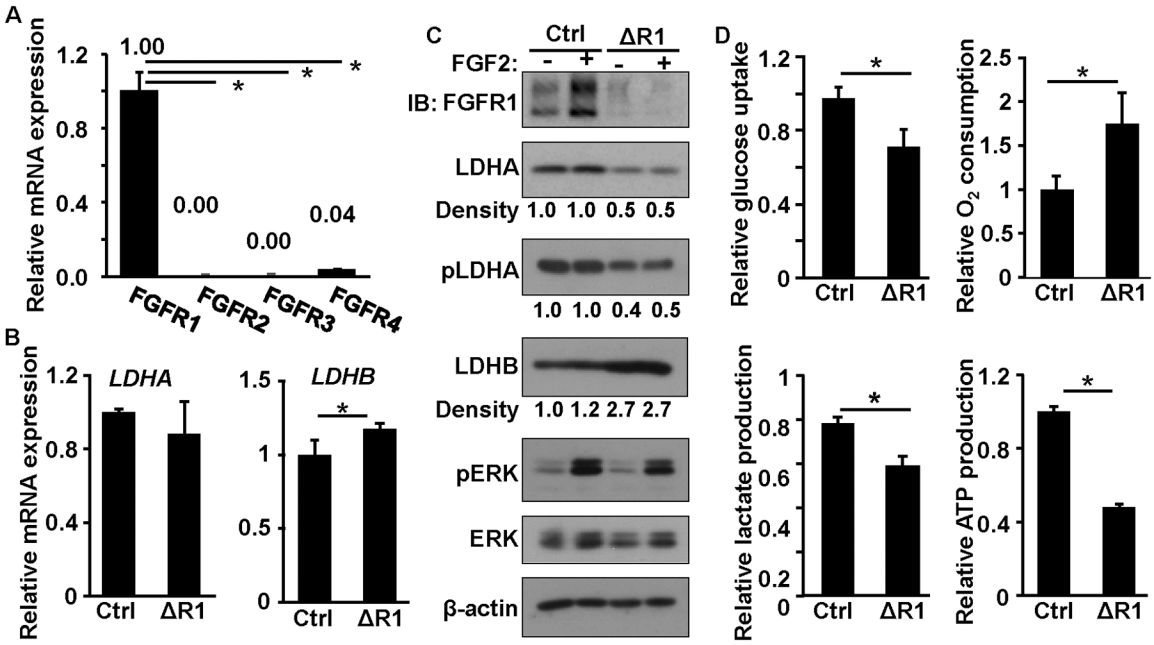

Fig. 4. Ablation of FGF signaling suppresses aerobic glycolysis and promotes oxidative phosphorylation in DU145 cells

A&B. Real-time RT-PCR analyses of FGFR and LDH isoform expression. **C.** Western blot of LDHA and LDHB expression. **D.** Comparison of glucose uptake, oxygen consumption, and lactate and ATP production. Ctrl, control; ΔR1, DU145$^{\Delta R1}$; *, $P < 0.05$; pLDHA, phosphorylated LDHA; pERK, phosphorylated ERK1/2; pAKT, phosphorylated AKT; β-actin was used as a loading control.

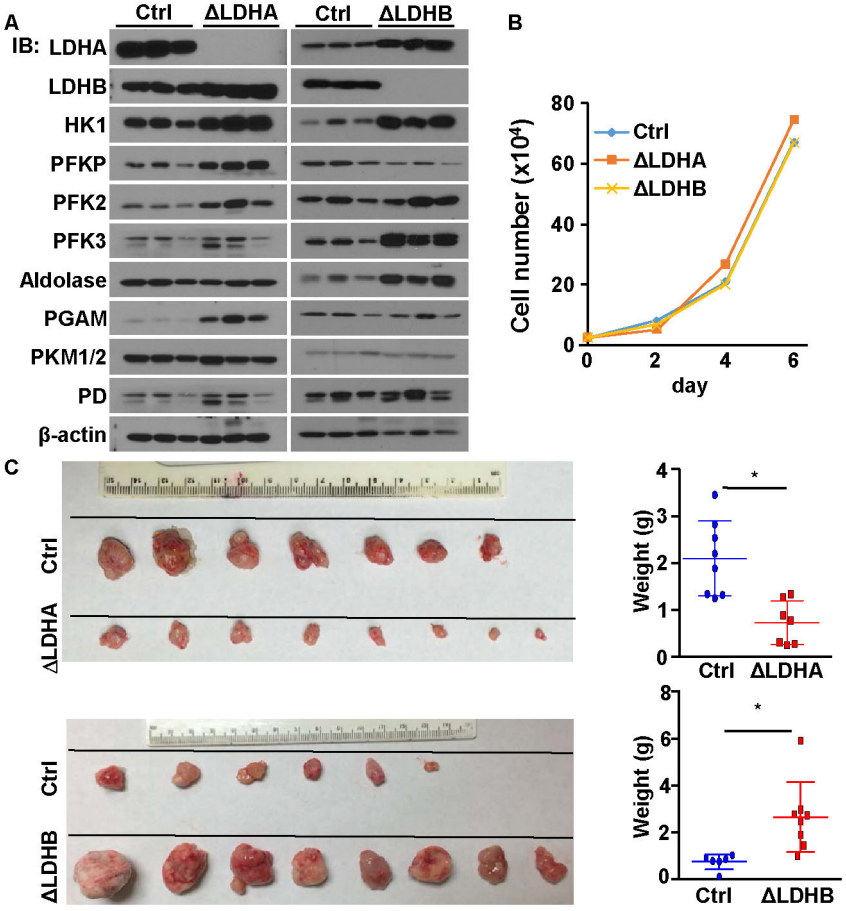

Fig. 5. LDHA ablation reduces, and LDHB ablation enhances, the tumorigenicity of DU145 cells

A, Western blot of the expression of enzymes related to aerobic glycolysis. **B.** The indicated DU145 cells ($2x10^4$) were plated on 6-cm dishes. Cell numbers were counted every other day. **C.** Xenografts derived from the indicated control DU145 cells. Note that the ΔLdha and ΔLdhb tumors were harvested at different days, because the ΔLdhb tumors reached the limit of tumor burden earlier than the ΔLdha tumors. The average xenograft weight was calculated from all individual xenografts and is presented in the right panels. ΔLDHA, $DU145^{\Delta Ldha}$; ΔLDHB, $DU145^{\Delta Ldhb}$; Ctrl, control DU145 cells; HK1, hexokinase 1; PD, pyruvate dehydrogenase.

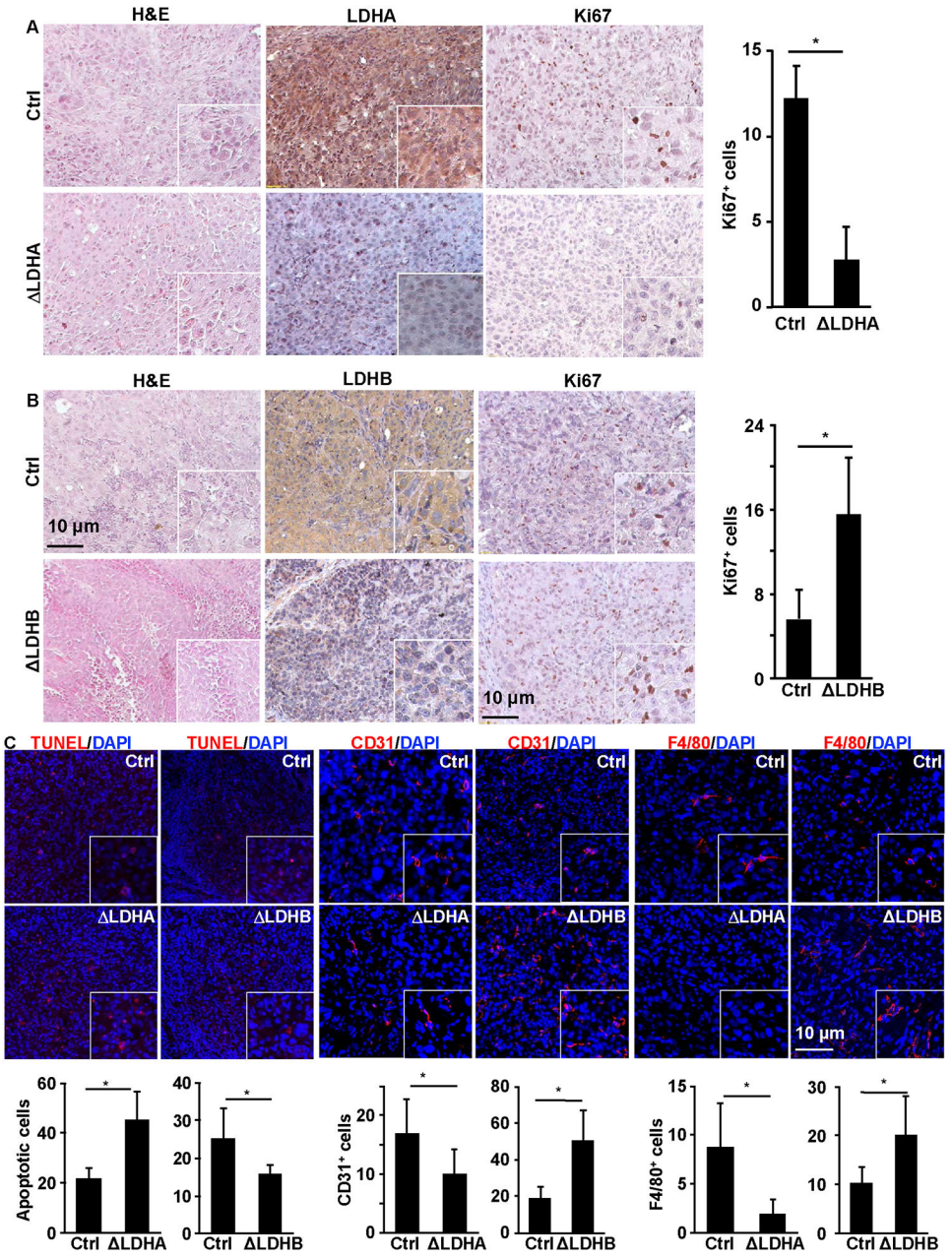

Fig. 6. Differential impacts of LDHA and LDHB on cell survival, angiogenesis, and inflammation in PCa xenografts

A&B. H&E and immunohistochemically staining. The numbers of Ki67$^+$ cells per viewing area were calculated from 20 viewing areas per tumor from six pairs of tumors and presented as the mean ± standard deviation in the right panels. **C**, Tissue sections of the xenografts were immunostained with TUNEL, anti-CD31, or anti-F4/80 antibodies as indicated. The numbers of positively stained cells per viewing area were calculated from 25 viewing areas from six pairs of tumors and presented as the mean ± standard deviation.

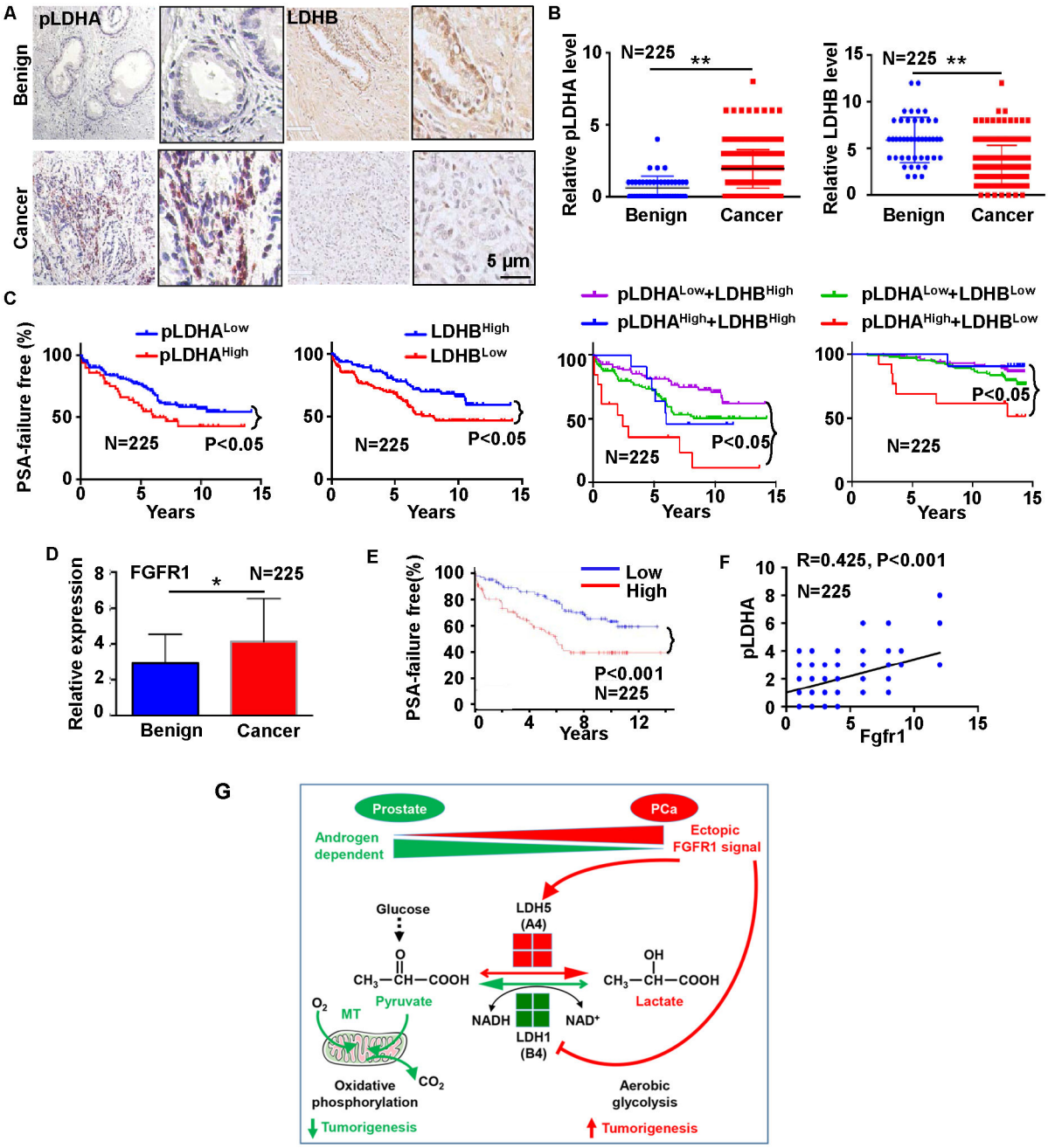

Fig. 7. High pLDHA and low LDHB expression predicts poor prognosis in patients with PCa

A. Representative images of immunochemical staining of pLDHA and LDHB in the MGH PCa TMA. **B**. Statistical analyses of the expression of LDHA and LDHB in PCa and benign prostate. **C**. PSA failure-free survival time in patients with low versus high phosphorylated LDHA a LDHB expression. **D**. Statistical analyses of FGFR1 in benign and cancer tissues. **E.** PSA failure-free survival time in patients with low versus high *FGFR1* expression. **F**. Pearson correlation of *Fgfr1* and pLDHA in the PCa TMA. **G**. Model of ectopic FGFR1 signaling in reprograming cell metabolism and promoting tumorigenesis.